Reinforced carbon foams prepared by chemical vapor infiltration: A process modeling approach

Gerard L. Vignoles, Cécile Gaborieau, Sophie Delettrez, Georges Chollon, Francis Langlais

Elsevier Editorial System(tm) for The International Conference on Metallurgical Coatings and Thin Films
Manuscript Draft

Manuscript Number: ICMCTF_2008-D-08-00043R1

Title: Reinforced carbon foams prepared by chemical vapor infiltration: a process modeling approach

Article Type: Full Length Article

Section/Category: Symposium B1-B4: Hard Coatings and Vapor Deposition Technology

Keywords: Pyrocarbon; Carbon foams; Chemical Vapor Infiltration; Modelling

Corresponding Author: Pr. Gerard L Vignoles,

Corresponding Author's Institution: University Bordeaux 1

First Author: Gerard L Vignoles

Order of Authors: Gerard L Vignoles; Cécile Gaborieau, M. D.; Sophie Delettrez, M. D. ; Georges Chollon, Ph. D. ; Francis Langlais, Ph. D.

Abstract: Carbon foams are attractive potential materials for shock insulation in extremely high temperatures; but the mechanical properties of the as-prepared foams are too low. Chemical Vapor Infiltration (CVI) of carbon or refractory ceramics is an interesting solution to over-come this drawback. However CVI itself contains several issues in terms of material quality. The thickness and nanostructure of the reinforcing deposit has to be uniform throughout large samples; achieving this goal through the control of processing parameters requires a sound knowledge of the process physico-chemistry. In that context, process modeling may bring some useful guidelines.
The presented work focuses on the deposition of pyrocarbon from pure propane in carbon foam samples with ~ 96% initial porosity, the treatment being stopped when porosity reaches ~85%. Depending on the chosen nanotexture of pyrocarbon, some infiltration gradi-ents may appear in the samples. The modeling is aimed at determining the importance of gas diffusion and deposition kinetics during deposition.
One of the elements of the model is the evolution of the internal surface area and aver-age pore diameter with the infiltration. This has been determined by X-ray computed micro-tomography (CMT) and 3D image analysis featuring a simulation of structure growth.
Previous studies on pyrocarbon deposition have allowed building a simplified chemi-cal mechanism featuring maturation, i.e. gas-phase hydrocarbon pyrolysis leading to reaction intermediates, and deposition of the latter. Combining this chemical model with the resolution of balance equations at reactor-scale and sample scale, and inserting the previously deter-mined structure evolution model brings a complete modeling frame that compares favorably with experimental results. A discussion of the interplay between transport and matura-tion/deposition kinetics is given, as a guideline for the choice of optimal infiltration parame-ters.

ICMCTF 2008 paper ICMCTF_2008-D-08-00043

Title: Reinforced carbon foams prepared by chemical vapor infiltration: a process modeling approach
G. L. Vignoles et al.

Replies to the referee's comments :

Reviewer #1:
1. Is it a new and original contribution?
Almost
2. Are all illustrations and tables necessary and adequate?
Yes, they are. But minor revision is necessary.
3. Is the summary adequate and informative?
No, it isn't. I think the second paragraph of "Summary" should be placed in the section "Discussion"
I have changed the title of the last section in "Summary and Outlook", which is more appropriate; as a consequence I didn't move the last paragraph that you have mentioned. Moreover I have added a couple of extra sentences which give other perspectives to the work.

4. Please list any further comments here:
Since the same modelling methodology has been used to simulate synthesis of Carbon/carbon composites by the authors and others, modelling details are not presented in the paper. Maybe for researchers in the field of carbon foams, it is difficult to understand the paper. From this point of view, the authors should give more details in the section of "modelling" if the paper is accepted.
I try to do so, but there is a length limitation which precludes an extensive description.
I have added sentences on the number of species and equations in the detailed 1D model, on the incorporation of diffusion and convection in the 1D mass balance, a balance equation for the 2D model, etc …

The authors present experimental results of carbon foams reinforced by pyrocarbon coatings of various microstructures. Modelling and simulation of ICVI processes are also performed in order to determine the competition of gas diffusion and deposition kinetics. X-ray CT is introduced to measure the evolution of surface area of carbon foams with progressive carbon deposition. The authors' work shows the contribution of modelling to up-scaling of process. Comments are given below.

1.Abstract is over presented. One paragraph is enough.
The new abstract is now shorter.

2.How about the effect of reinforcement on mechanical and thermal properties of carbon foams? Do you have additional measurement results of mechanical or thermal properties.
These properties are being measured but are the object of another communication. This is indicated at the end of the text.

Details of 3D image process or more information should be estimated because the pixel size of X-ray CT is almost in the same order of magnitude as carbon deposition rate (per hour).

Actually, indirect information is provided by the spacing of points on fig. 4, which corresponds to a single dilation step at a time. Note that Fig. 4 has been changed : i) there was a scale factor mistake for the 100 ppi sample, ii) the “end points” are also reported.

4.The reaction mechanism involved in your "weakly coupled CVI model" should be given in the format of chemical reactions. For audiences, it will be easy to understand it.

I had not chosen to do so because it is an *ad-hoc* model and not a truly chemical model. Table 2 is now completed with a sketch of the reaction mechanism in the text.

5.It seems Table 3 mentioned in the text is not presented at the end of the paper. Has it been merged into Table 2?

You are right. I have modified the text in relation with this.

6. More details of the "weakly coupled CVI model" should be given. For example, distinguish the molar volume difference between WAL carbon and HAL carbon or not? It will affect the calculation of carbon deposition rates.

The molar volume difference has been accounted for (see table 2). Now the values are given.

7.3D plots can not show the experimental data clearly, maybe double y plots are better.

Actually I had double y plots first and they seemed much more difficult to read to me than those.

Reviewer #2: This paper deals with a novel approach to produce advanced foam material. I found nothing unfavorable in this paper, and recommend that this paper should be published as it is.

Thank you very much !

*** Manuscript**

Paper Number: B3-1-1
Title of Paper: Reinforced carbon foams prepared by chemical vapor infiltration : a process modeling approach

Corresponding Author: Gerard L. Vignoles

Full Mailing Address: LCTS, UMR 5801 CNRS-UB1-Safran-CEA, 3 allée La Boëtie, Domaine Universitaire, 33600 Pessac, France.
Telephone: (+33) 556 844 734
Fax: (+33) 556 841 225
E-mail: vinhola@lcts.u-bordeaux1.fr

Estimation of the length of the manuscript
(the pages of the manuscript should be numbered)

			Number of words
Number of Pages	9	× 250	2250
Number of Tables	2	× 150	300
Number of Figures	6	× 150	900
TOTAL NUMBER OF WORDS =			3450

Reinforced carbon foams prepared by chemical vapor infiltration: a process modeling approach

G. L. Vignoles[a], C. Gaborieau[b], S. Delettrez[c], G. Chollon[c], F. Langlais[c]

[a] *Univ. Bordeaux 1, LCTS, UMR 5801 CNRS-UB1-Safran-CEA, 3 Allée La Boëtie, 33600 Pessac, France*
[b] *CEA, LCTS, UMR 5801 CNRS-UB1-Safran-CEA, 3 Allée La Boëtie, 33600 Pessac, France*
[b] *CNRS, LCTS, UMR 5801 CNRS-UB1-Safran-CEA, 3 Allée La Boëtie, 33600 Pessac, France*

ABSTRACT

Carbon foams are attractive potential materials for shock insulation in extremely high temperatures; but the mechanical properties of the as-prepared foams are too low. Chemical Vapor Infiltration (CVI) of carbon or refractory ceramics is an interesting solution to overcome this drawback.

The presented work focuses on the deposition of pyrocarbon from pure propane in carbon foam samples with ~ 96% initial porosity, the treatment being stopped when porosity reaches ~85%. Depending on the chosen nanotexture of pyrocarbon, some infiltration gradients may appear in the samples.

A modeling approach, aimed at determining the importance of gas diffusion and deposition kinetics during deposition, is presented, validated and discussed. The model features (i) determination of internal surface area during infiltration based on X-ray CMT and 3D image analysis, (ii) a simplified chemical model for hydrocarbon pyrolysis and pyrocarbon deposition, (iii) resolution of balance equations at reactor-scale and sample scale. The model results compare favorably with experimental data. A discussion of the interplay between transport and maturation/deposition kinetics is given, as a guideline for the choice of optimal infiltration parameters.

Key words : Pyrocarbon; Carbon foams; Chemical Vapor Infiltration; Modeling

INTRODUCTION

Carbon foams are used in a variety of applications, among which thermal [1] and electrical [2] transfer devices, as well as thermal insulators, *e.g.* for atmospheric re-entry thermal protection structures [3]. Vibration damping [4] and shock absorption [5] properties also indicate applications in ballistic containment cases, especially at high temperatures. In this last case, the mechanical properties of the as-prepared foams may be too low for a direct use; in order to circumvent this drawback, one has to reinforce the carbon foam structure. Actually, following this analysis, carbon foams have been frequently used as mere templates for the preparation of metal [6] or ceramic [7,8] foams. In the present case, the carbon foam will be a template for a pyrocarbon foam, *i.e.* the reinforcement is pyrocarbon, as deposited by Isothermal, isobaric Chemical Vapor Infiltration (I-CVI) [9,10].

As it is well known [11,12], pyrocarbon (*pyC*) is a pre-graphitic form of carbon deposited by chemical vapor deposition (CVD) or by CVI. Precursor gases are hydrocarbons possibly diluted in hydrogen, their thermal decomposition yields complex mixtures of radical and molecular species, which eventually react with a substrate and give a solid carbon deposit. The nanotexture of the pyrocarbon is known to depend strongly on the processing parameters, among which the gas composition, the total pressure and temperature, the residence time and the reactor surface/volume ratio [13-21]. This is an important issue since their mechanical and thermal properties, as well as their graphitizability, rely on the nanotexture [12,22].

In addition to the control of pyrocarbon nanotexture, the question of deposit uniformity is a crucial point in CVI processing [23]. Indeed, when performed in isothermal and isobaric conditions, the deposition reaction provokes an internal reactant depletion, which eventually leads to a lesser deposit thickness in the center of the porous medium. This competition between reaction and transport [24] has to be carefully evaluated in order to perform process scale-up operations.

In this work, the reinforcement of a polymer-derived carbon open-cell foam by pyrocarbon, using CVI from pure propane, is studied experimentally. Working conditions for the deposition of two forms of pyrocarbon are obtained. The deposit thickness homogeneity is measured and some slight gradients are present in the samples. A modeling strategy is then proposed in order to account for these phenomena; then, guidelines for an optimal process are given.

EXPERIMENTAL

Two kinds of vitreous carbon foam samples were used, with distinct pore sizes. One has 60 *ppi* (pores per inch) and the other 100 *ppi*. The pore volume fractions are respectively 97.7 ± 0.8% and 96.2 ± 0.3%. The samples were cylindrical with 10 *mm* in height and diameter.

The experimental setup consists in a low-pressure hot-wall tubular CVD reactor, previously described in [21,25]. The tube diameter was 34 *mm* and the hot zone size (defined with a precision of 10 *K*) is 30 *mm*. The maximal temperature is 1100°*C* and the pressure ranges between 2 and 10 *kPa*. Pure propane was used as an input gas; the residence time in hot zone may vary between 0.05 *s* and 5 *s*.

Using pure propane as a precursor, it is possible to perform deposition of three distinct kinds of laminar pyrocarbons. When increasing either the residence time or the process temperature, one obtains successively [26]: *i*) Granular and Columnar (GL and CL) pyrocarbons, collectively denominated Rough Laminar (RL), *ii*) Weakly anisotropic laminar (WAL), also known as Smooth Laminar (SL), and *iii*) Highly Anisotropic Laminar (HAL), also known as Regenerative laminar (ReL) [27], which had long been mistaken for RL. After an optimization campaign, two sets of control parameters were fixed for the respective deposition of WAL (SL) and HAL (ReL) pyrocarbons: temperature 1323 *K* and pressure 5 *kPa* for both, and residence time 0.2 *s* and 3 *s* respectively.

The infiltrated samples were characterized by polarized light Raman microscopy [26] in order to assess the nanotexture; the deposit thickness distribution throughout the foam sample has been measured by optical microscopy. Also, the foam samples have been monitored by X-ray microfocus computerized tomography (Phoenics X-ray Nanotome with pixel size after reconstruction equal to 3 or 5 μm). The 3D images have been processed in order to extract several geometrical parameters: internal surface area, average cell size, hydraulic diameter and ligament width. The density and porosity have been measured experimentally by Archimedes method and helium pycnometry. The internal surface area has been measured by performing short-time infiltrations in reaction-limited regimes and dividing the overall mass gain rate by the rate per unit area obtained in CVD experiments on plain substrates.

RESULTS

Table 1 is a summary of some geometrical properties obtained either from experimental determination or by X-ray CMT image analysis. Figure 1 is a visualization of the CMT data before and after infiltration.

The growth rates are neatly distinct in WAL pyC and HAL pyC deposition conditions: they are respectively 4 and 13 $\mu g/min/cm^2$. The deposit thickness profiles are reported on Figure 2. One can see that the deposit uniformity is rather satisfying in the case of WAL pyC deposition, for which the rate is neatly lower; on the other hand, HAL pyC deposition yields an appreciable deposit thickness gradient. In correlation with this, there is a neat discrepancy between the effective deposition rate in CVI conditions (13 $\mu g/min/cm^2$) and the apparent deposition rate in CVD conditions (33 $\mu g/min/cm^2$).

MODELING

The modeling strategy is decomposed in three steps, as dictated by the involved phenomena. The first part concerns the evolution of the concentrations of the various hydrocarbons in the tubular furnace, as a result of the propane pyrolysis; the second part combines propane pyrolysis and heterogeneous deposition inside the foam, and the third one deals with

the structural evolution of the foam under deposition conditions. Indeed, there is a weak coupling between each of these sub-models, because (i) the available surface for heterogeneous deposition is low enough, so that the surrounding gas phase is not deeply affected by them (a situation termed “weakly coupled CVI” or wc-CVI [19]), and (ii) the structural evolution is very slow, which enables one to consider that the gas phase is in pseudo-steady state at every infiltration step [28].

The reactor-scale model is based on a 1D steady-state resolution of the mass and species balance equations, featuring a semi-detailed mechanism for propane pyrolysis [19]. There are 41 species (from C1 : CH_4, CH_3, etc… to C10 : $C_{10}H_8$) and 133 reactions in this mechanism. The measured temperature profile has been imposed to the gas phase. Indeed, the gas velocity is low enough to ensure a correct thermal transfer in radial direction, and the pyrolysis reactions do not consume or produce any appreciable amounts of heat: accordingly, the heat balance resolution may be safely switched off. Mass balance equations feature convection and diffusion, since both phenomena are in clear competition in the considered case. The computations were carried out using the Cantera software [29].

As a typical result, Figure 3 is a plot of the partial pressures of some species groups along the reactor length coordinate. The gas-phase maturation phenomenon is evidenced: the initial decomposition of propane gives first-generation species, most in C1 (methyl radical) and C2 (ethane, ethene); then, later acetylene and benzene appear; finally, higher molecular-weight species occur. The transition from WAL to HAL is linked to this last step [19,21]. In order to perform subsequent CVI computations, the homogeneous reaction scheme is simplified, with a few lumped species and apparent reactions; the scheme is listed in Table 2. Then, the heterogeneous reaction rates are fitted from those species concentrations and CVD experiments; Table 2 also lists the heterogeneous reactions retained, expressed in terms of sticking coefficients. Though this overall lumped mechanism has no precise actual chemical meaning, it is represented as the following equivalent scheme:

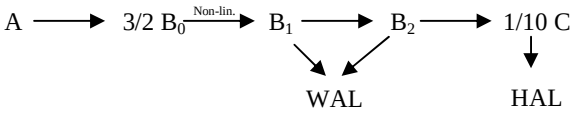

(1)

The complete kinetic scheme may be introduced in a 2D axisymmetrical mass balance solver for foam consolidation. The gas transport may rely on viscous flow, ordinary (binary) diffusion, and rarefied gas flow (Knudsen diffusion) [30]. In the present case, since the gases may freely flow around the porous sample, no appreciable pressure buildup appears: consequently, viscous flow is rather negligible with respect to the other transport modalities, as usual in isothermal CVI. The equations are, noting R_i the production rate of species i:

$$\mathrm{div}\left(-D_i^{por}\nabla C_i\right)=\varepsilon R_i^{\mathrm{hom}}-\sigma_v R_i^{het}$$
$$\frac{dh}{dt}=\Omega_s\sigma_v R_i^{het} \qquad (2)$$

The effective diffusivities D_i^{por} and the internal surface area σ_v, given as functions of the pore volume fraction ε (or of some other infiltration progress variable), have to be determined. In this goal, the 3D CMT images have been used. Deposit growth has been simulated by successive solid phase dilations starting from the raw foam images; the resulting blocks have been processed for the determination of the internal surface area and of the effective binary and Knudsen diffusivities, by use of a Monte-Carlo/random walk algorithm [31-34]. Fig. 4 is a plot of the determined laws. Every single dilation step (*i.e.* one pixel thickness) corresponds to a leap from one symbol to the next one on the curve. As a comparison, the values obtained for the actual infiltrated foams are reported, showing excellent agreement with the computed evolution: this is possible since the sticking probabilities are extremely low, thus preventing the foam from local (*i.e.* bubble-scale) depletion effects.

The temperature is assumed constant throughout the foam, since it lies in the reactor hot zone and the gas flow rate is moderate. The concentrations C_i^0 obtained as a result of the 1D code and given as a function of the height in the hot zone are not prescribed directly as

input values at the foam sample boundaries; instead, a Fourier-like boundary condition is given:

$$-D_i^{por}\nabla C_i \cdot n = \frac{D_i^{free}}{\delta}\left(C_i^0 - C_i\right) \quad (3)$$

This is related to the fact that the foam is so reactive that it is able to deplete the reactant concentration around it on some boundary layer thickness δ; in our case δ has been fixed to the difference between the reactor radius and the preform radius. The effective diffusion coefficient in the porous medium is given by [35]:

$$D_i^{por} = \varepsilon^{5/3} D_i^{free} \quad (4)$$

Then, resolution of the gas mass balances yields the gas partial pressures and deposition rate fields in the sample, as well as the effective gas fluxes at the foam boundaries. Computation of the latter helps to confirm the hypothesis of weakly coupled CVI [20] in the case of WAL pyC deposition, and to infirm it in the case of HAL pyC deposition. The time evolution of the sample density is given by solving the solid mass balance equations, using the values of the deposition rates computed before. All 2D numerical computations have been carried out on a commercial finite element code [36].

DISCUSSION

Figs. 5 and 6 show the spatial repartition of the computed deposit rates throughout the 60 *ppi* foam sample, as compared to the experimental values, in the two chosen deposition conditions. The agreement is good, both in global deposition rate and in deposit thickness gradients, even though the gradient is slightly underestimated in the case of HAL pyC deposition.

One of the most interesting facts that should be noted from this modeling study is that in the case of WAL pyC deposition, the gas-phase maturation chemistry has a beneficial effect on the deposit homogeneity. Indeed, the deposition rate from the propane molecule is very low compared to the rate from the products of its cracking. The high reactivity of these

products would enhance depletion effects, because of an adverse reaction/diffusion ratio, but since they are produced by a relatively slow decomposition reaction, they gain time to enter the pores. Such an effect had been discussed theoretically by Middleman [37]. It has been described experimentally in the case of methane pyrolysis for pyrocarbon infiltration [38], where in some cases it may lead to an inside-out infiltration. Here, since propane is much more reactive than methane, this is not the case.

On the other hand, and rather strikingly, this effect does not show up for HAL deposition. The reason is that the consumption of heavy (type C) species by deposition is fast with respect to the renewal rate by pyrolysis of lighter species (types B1 and B2).

Let us finally remark that the presented model yields, at least for these conditions, satisfactory results without having to refer explicitly to H inhibition [39]. Since there were large amounts and virtually no gradients of H_2 close to the sample from the 1D computations with detailed chemistry, any hydrogen inhibition effect is suspected to act homogeneously in the samples; thus, in our model, it may only appear through the absolute value of the fitted deposition rate constants.

SUMMARY AND OUTLOOK

Pyrocarbon-consolidated carbon foams have been prepared by I-CVI in an LPCVD apparatus; satisfying conditions for the deposition of either WAL or HAL pyrocarbon have been found. In order to scale up the processing conditions, a modeling procedure, based on a 1D detailed + 2D lumped chemistry model, has been set up and validated by comparison with these results. It shows that the deposition uniformity in WAL pyC deposition conditions is mostly linked to the existence of a gas-phase maturation phenomenon, which precedes the actual deposition. Because of this non-linear behavior, the model is beneficial in helping the engineer for the up-scaling of the process, *i.e.* when one considers infiltration of much thicker foam samples. In the case of HAL pyC deposition, the high heterogeneous reactivity of the

direct precursors (heavy hydrocarbons) results in a large deposit thickness gradient throughout the foam.

From the process modelling point of view, carbon foams are of special interest because they are porous media with moderate internal surface area values, and their structural evolution may be monitored with a good precision. In other words, they are like “model porous media”, which are particularly suited for the testing and validation of chemical deposition models, when one switches from CVD (very low surface area) to CVI (very high surface area).

Mechanical properties of the reinforced foams are currently under investigation [40]. The reinforcement of foams has also been envisaged with SiC deposits; the present study may be extended to this case: this is the aim of future work.

ACKNOWLEDGEMENTS

The authors wish to thank Commissariat à l’Energie Atomique (CEA) and Centre National de la Recherche Scientifique (CNRS) for support to S. D. through a Ph. D. grant.

LIST OF REFERENCES

1. N. C. Gallego and J. W. Klett, Carbon 41 (2003) 1461
2. Q.-W. Zhang, X. Zhoua and H.-S. Yang, J. Power Sources 125 (2004) 141
3. D. M. Spradling and A. R. Guth, Adv. Mater. and Processes 161(2003) 29
4. K. Maslov and V. K. Kinra, Mater. Sci. Eng. A 367 (2004) 89
5. E. Bruneton, C. Tallaron, N. Gras-Naulin and A. Cosculluela, Carbon 40 (2002) 1919
6. D. T. Queheillalt, Y. Katsumura, H. N.-G. Wadley, Scripta Materialia 50 (2004) 313
7. E. J. A. Pope, A. Almazan, K. Kratsch, J. Amer. Ceram. Soc. 74 (1991) 1722
8. T. L. Marbach, V. Sadasivuni, A. K. Agrawal, Combust. Sci. Tech. 179 (2007) 1901
9. R. Naslain and F. Langlais, Mater. Sci. Res. 20(1992) 145.
10. R. Naslain, F. Langlais, G. L. Vignoles and R. Pailler, Ceram. Eng. Sci. Proc. 27(2) (2006) 373
11. J. C. Bokros, Chemistry and Physics of Carbon 5 (1969) 1

12. P. Loll, P. Delhaès, A. Pacault, A. Pierre, Carbon 15 (1977) 383

13. R.J. Diefendorf, in J. W. Mitchell, R. C. de Vries, and P. Cannon (eds.), "Reactivity of solids", (Wiley & sons, New York, 1969)

14. P. Lieberman and H.O. Pierson, Carbon 12 (1974) 233

15. B. Reznik and K. J. Hüttinger, Carbon 40 (2002) 617

16. X. Bourrat, J.-M. Vallerot, F. Langlais, G. L. Vignoles, L'Actualité Chimique 295-296 (2006) 57 (in French)

17. X. Bourrat, F. Langlais, G. Chollon and G. L. Vignoles, J. Braz. Chem. Soc. 17 (2006) 1090

18. C. Descamps, G. L. Vignoles, O. Féron, F. Langlais and J. Lavenac , J. Phys. IV France 11 (2001) Pr3-101

19. C. Descamps, G. L. Vignoles, O. Féron, F. Langlais and J. Lavenac, J. Electrochem. Soc. 148 (2001) C695

20. N. Reuge, G. L. Vignoles, H. Le Poche, F. Langlais, Adv. Sci. Technol. 36 (2002) 259

21. G. L. Vignoles , F. Langlais, C. Descamps, A. Mouchon, H. Le Poche, N. Bertrand and N. Reuge, Surf. Coat. Technol. 188-189 (2004) 241

22. A. Oberlin, Carbon 22 (1984) 521

23. I. Golecki, Mater. Sci. Eng. Reports R20 (1997) 37

24. G. L. Vignoles, Adv. Sci. Technol. 50 (2006) 97

25. F. Langlais, H. Le Poche, J. Lavenac and O. Féron : Electrochem. Soc. Procs Vol. PV 2005-09 (2005) 73

26. J.-M. Vallerot, X. Bourrat, A. Mouchon and G. Chollon, Carbon 44 (2006) 1833

27. X. Bourrat, A. Fillion, R. Naslain, G. Chollon and M. Brendlé, Carbon 40 (2002) 2931

28. N. Reuge and G. L. Vignoles, J. Mater. Process. Technol. 166 (2005), 15

29. D. G. Goodwin, "Cantera: Object-Oriented Software for Reacting Flows" (2004), www.cantera.org (visited 2008)

30. J. Y. Ofori and S. V. Sotirchos, Ind. Eng. Chem. Res. 35 (1996) 1275

31. G. L. Vignoles, J. de Phys. IV C5 (1995) 159

32. O. Coindreau and G. L. Vignoles, J. Mater. Res. 20 (2005) 2328.

33. G. L. Vignoles, O. Coindreau, A. Ahmadi and D. Bernard, J. Mater. Res. 22 (2007) 1537

34. Ch. Mulat, P. Baylou, Ch. Germain, G. L. Vignoles, These proceedings, to appear in Surf. Coat. Technol. (2008)

35. G. L. Vignoles, J.-M. Goyhénèche, P. Sébastian, J.-R. Puiggali, J.-F. Lines, J. Lachaud, P. Delhaès and M. Trinquecoste, Chem. Eng. Sci 61 (2006) 5336.

36. FlexPDE software, www.pdesolutions.com (visited 2008)

37. S. Middleman, J. Mater. Res 4 (1989) 1515.

38. W. G. Zhang, and K.J. Hüttinger ECS Proceedings PV 2003-08 (2003) 549

39. A. Li and O. Deutschmann, Chem. Eng. Sci. 62 (2007) 4976

40. S. Delettrez, G. Chollon, F. Langlais, "Carbon open-cell foams: CVD processing and characterization" in Proc. Carbon 2008, Nagano, Japan, June 2008.

TABLES

Sample	60 *ppi*, raw		60 *ppi*, consolidated		100 *ppi*, raw		100 *ppi*, consolidated	
	Exp.	Calc.	Exp.	Calc.	Exp.	Calc.	Exp.	Calc.
Density ($g.cm^{-3}$)	0.04 ± 0.0062		0.35		0.064 ± 0.0013		0.35	
Pore volume fraction	97.7 ± 0.8%	94.5 %	82.8 %	84 %	96.2 ± 0.27 %	96.3 %	81.4 %	87.2 %
Bubble size (μm)	650	800	-	800	500	650	-	650
Ligament width (μm)	-	20	110	130	-	18	80	60
Pore hydraulic diameter (μm)	-	1300	-	500	-	860	-	690
Internal surface area (cm^{-1})	29.6	19.5	38.2	62	52.1	30	87.3	100.4

Table 1. Morphological parameters for two foams, raw and consolidated by pyC CVI.

Species group	*Possible nature*
A	***A*** : C_3H_8
B	***B0*** : CH_4 , C_2H_4 and C_2H_6 ***B1*** : C_2H_2 ***B2*** : C_6H_6
C	PAHs : here, $C_{10}H_8$

	Balance	*Rate law (units are mol, m, J, K)*
	$\frac{\partial[A]}{\partial t} = -k_A[A]$	ln k_A = 33.817 – 318364/**R***T*
	$\frac{\partial[B_0]}{\partial t} = -1.5\frac{\partial[A]}{\partial t}$	
	$\frac{\partial[B_1]}{\partial t} = k_{11}[B_0] + k_{12}[B_0]^2 + k_{14}[B_0]^4$	ln k_{11} = 36.465 – 427159/**R***T* ln k_{12} = 44.063 – 490824/**R***T* ln k_{14} = 25.448 – 240422/**R***T*
	$\frac{\partial[B_2]}{\partial t} + 10\frac{\partial[C]}{\partial t} = k_2[B_1]$	ln k_2 = 23.087 – 242193/**R***T*
	$\left.\frac{dh}{dt}\right\|_{WAL} = 2\Omega_{WAL}k_{WAL}([B_1] + 3[B_2])$	k_{WAL} (1323 K) = 3.6 10^{-4} $m.s^{-1}$ (st. prob. 2.10^{-6}) Ω_{WAL} = 5.6 10^{-6} $m^3.mol^{-1}$
	$\frac{\partial[C]}{\partial t} = -k_3[B_2]$	ln k_3 = 20.374 – 208831/**R***T*
	$\left.\frac{dh}{dt}\right\|_{HAL} = 10\Omega_{HAL}k_{HAL}[C]$	k_{HAL} (1323 K) = 7.8 10^{-3} $m.s^{-1}$ (st. prob. 7.10^{-5}) Ω_{HAL} = 6.0 10^{-6} $m^3.mol^{-1}$

Table 2. Lumped chemical model for WAL and HAL pyC deposition at 5 *kPa*, 1323 *K*

FIGURE CAPTIONS

Figure 1. Visualization of foam samples from X-ray CMT data. All extracts have the same size and are 0.35 mm in depth. a) 60 *ppi*, raw ; b) 60 *ppi*, consolidated; c) 100 *ppi*, raw , d) 100 *ppi*, consolidated.

Figure 2. Infiltration profiles for a 60 *ppi* foam in conditions for WAL and HAL pyC deposition.

Figure 3. Computed mole fraction profiles for lumped species in WAL and HAL deposition conditions. A : C_3H_8 ; B0 = CH_4+C_2H_4+C_2H_6 ; B1 = C_2H_2 ; B2 = C_6H_6; C = $C_{10}H_8$.

Figure 4. Surface area *vs.* pore volume fraction, as computed from X-ray CMT images and image dilation.

Figure 5. Computed pore volume fraction field through a 60 *ppi* foam in WAL pyC deposition conditions

Figure 6. Computed pore volume fraction field through a 60 *ppi* foam in HAL pyC deposition conditions

Figure 1

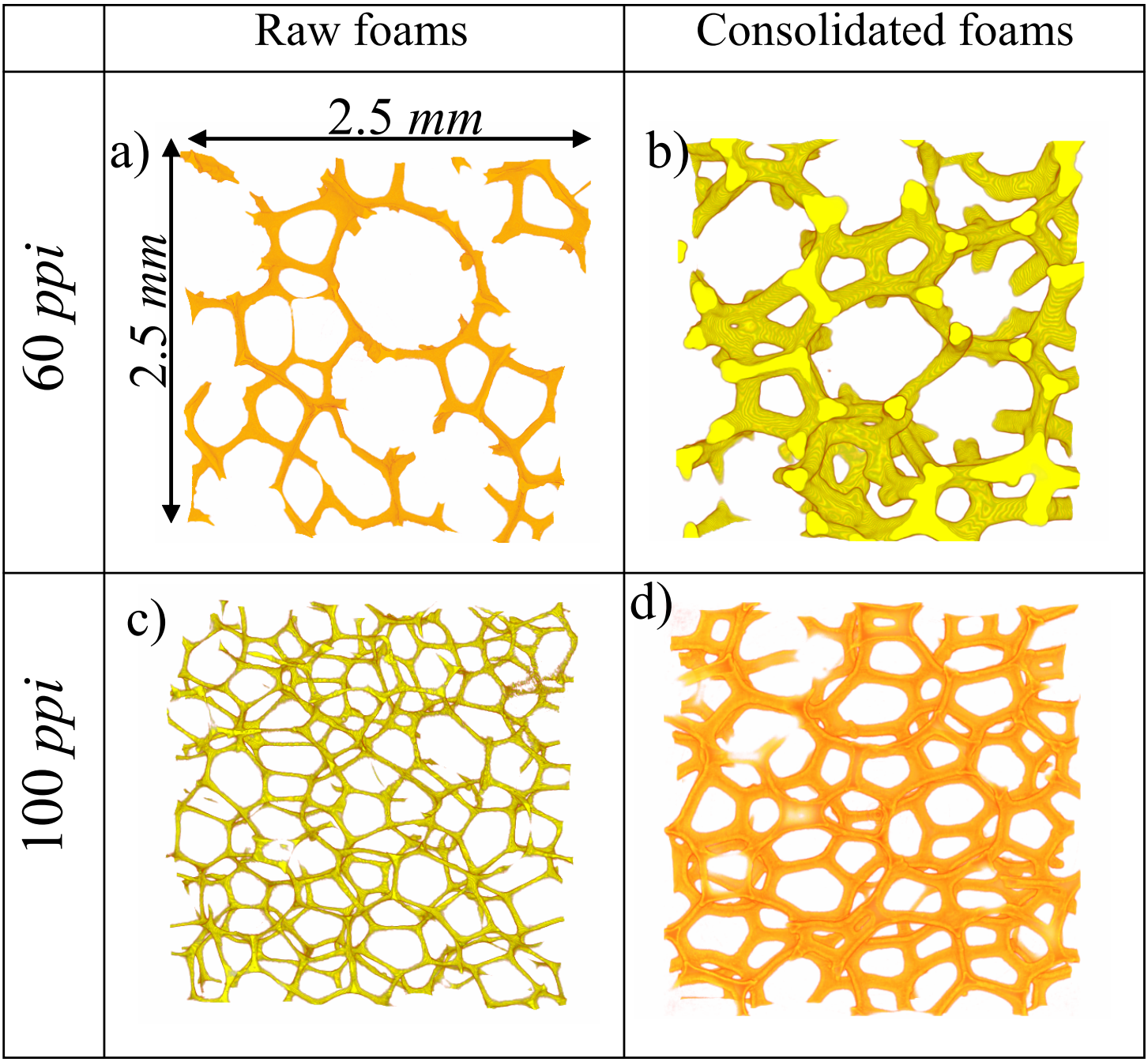

Figure 2

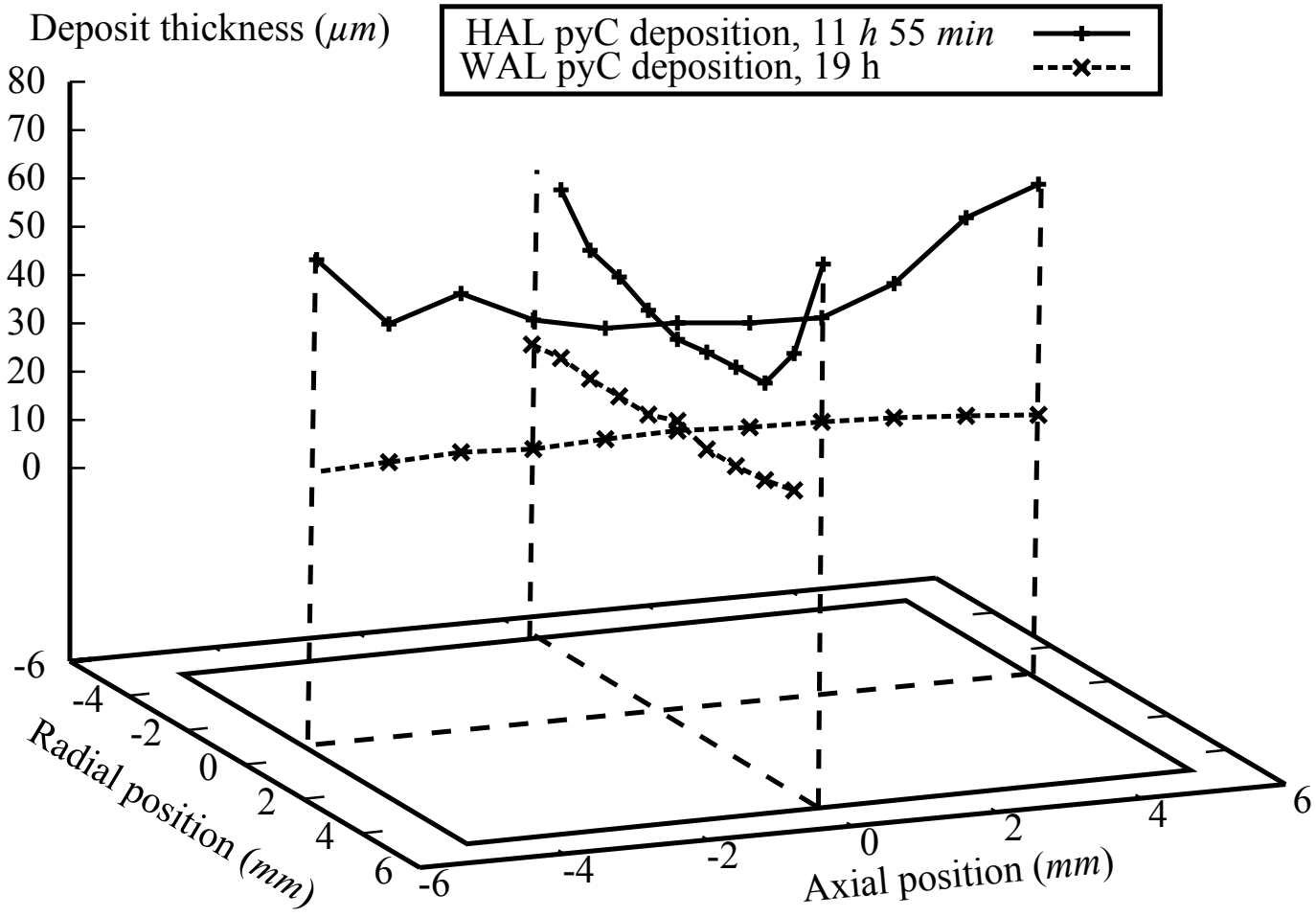
Deposit thickness (μm)
HAL pyC deposition, 11 *h* 55 *min*
WAL pyC deposition, 19 h
80
70
60
50
40
30
20
10
0
-6
-4
-2
0
2
4
6
Radial position (*mm*)
-6
-4
-2
0
2
4
6
Axial position (*mm*)

Figure 3

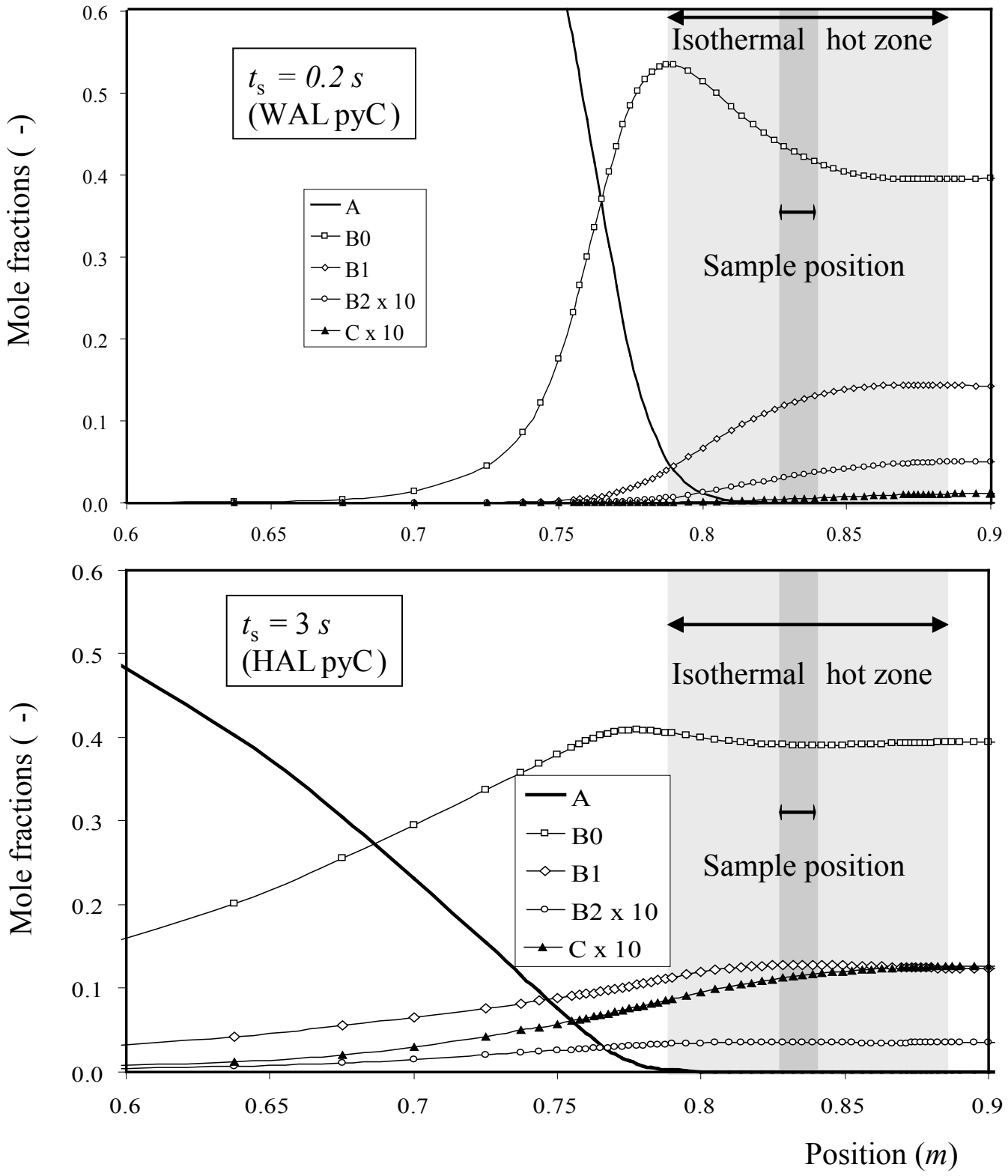
t_s = 0.2 s
(WAL pyC)
A
B0
B1
B2 x 10
C x 10
Isothermal hot zone
Sample position
Mole fractions (-)
t_s = 3 s
(HAL pyC)
Position (m)

Figure 4

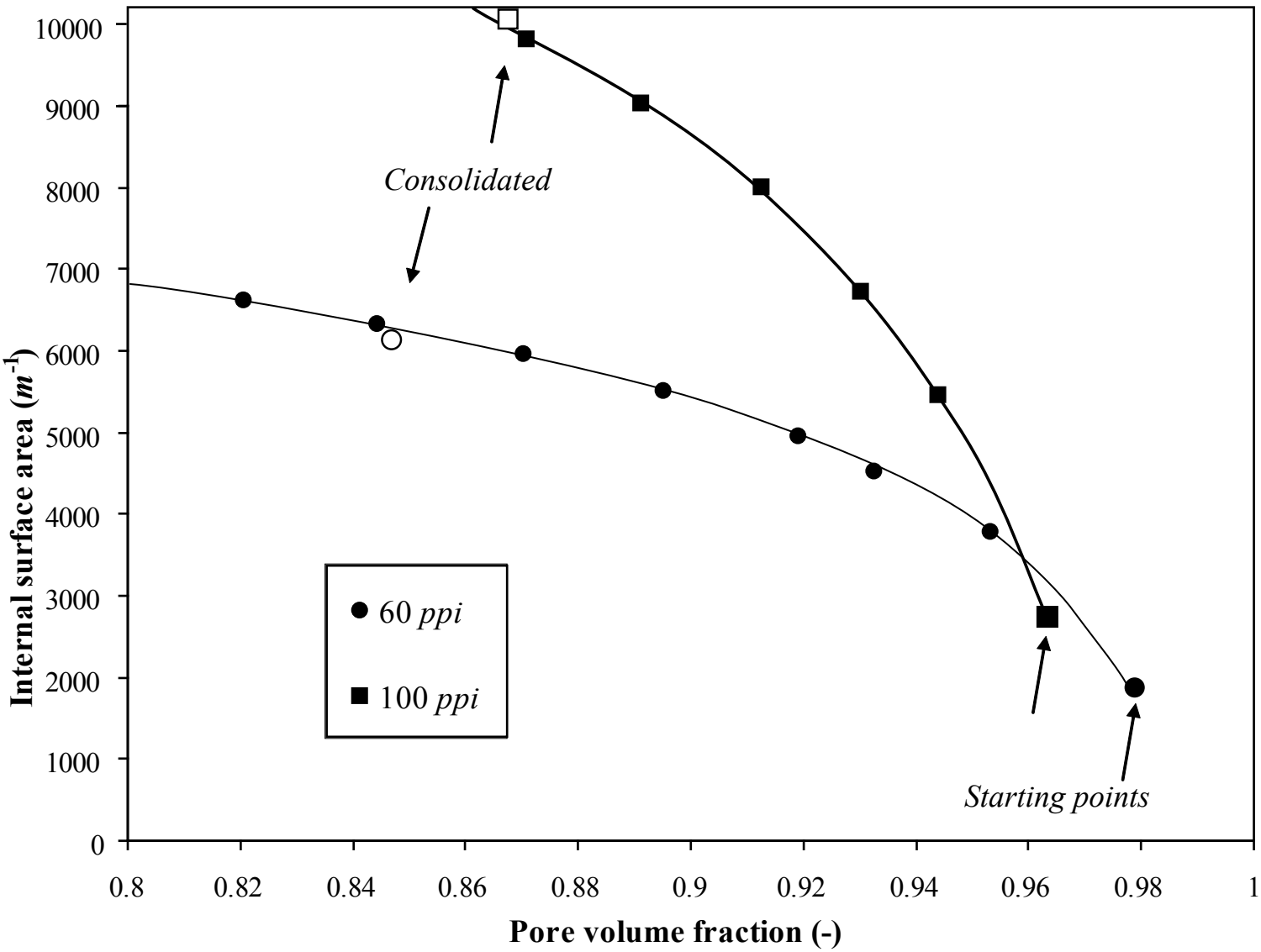
10000
9000
8000
7000
6000
5000
4000
3000
2000
1000
0
Internal surface area (m^{-1})
0.8
0.82
0.84
0.86
0.88
0.9
0.92
0.94
0.96
0.98
1
Pore volume fraction (-)
Consolidated
60 ppi
100 ppi
Starting points

Figure 5

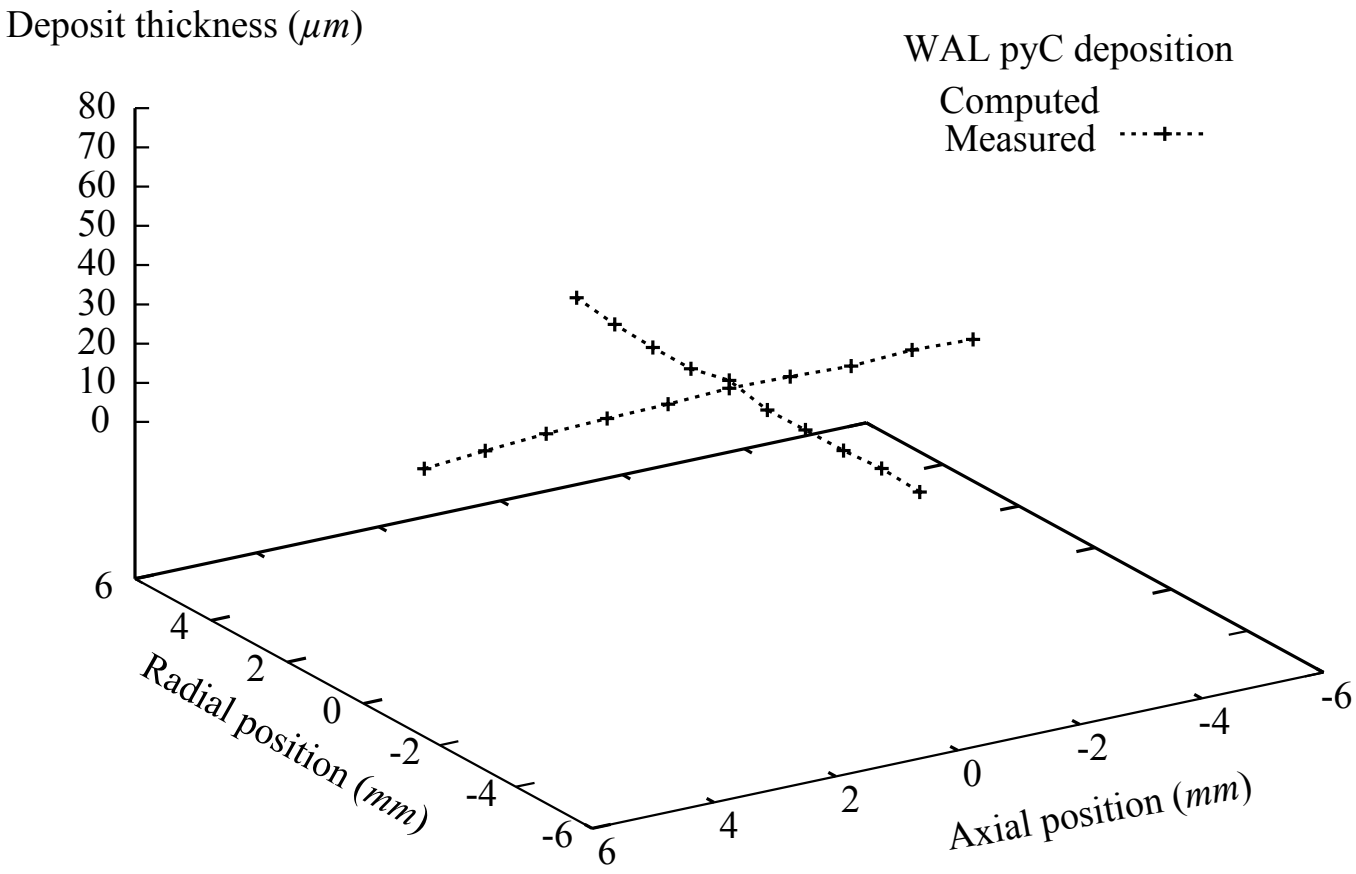
Deposit thickness (μm)
WAL pyC deposition
Computed
Measured
80
70
60
50
40
30
20
10
0
6
4
2
0
-2
-4
-6
Radial position (mm)
6
4
2
0
-2
-4
-6
Axial position (mm)

Figure 6

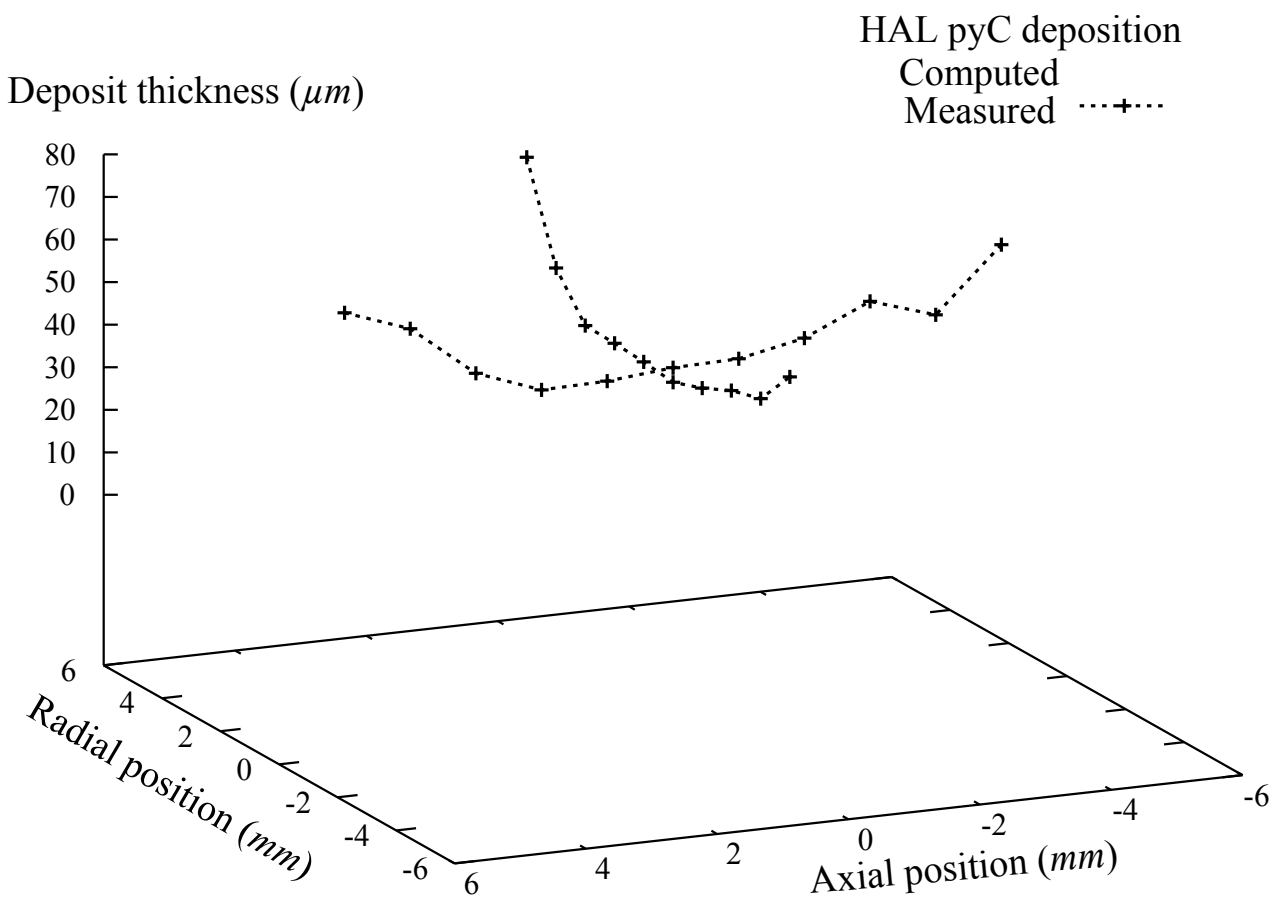
HAL pyC deposition
Computed
Measured
Deposit thickness (μm)
80
70
60
50
40
30
20
10
0
6
4
2
0
-2
-4
-6
Radial position (mm)
6
4
2
0
-2
-4
-6
Axial position (mm)